

# Numerical Simulation of the Aluminum Alloys Solidification in Complex Geometries

Eliseu Monteiro, Abel Rouboa\*

Engineering Department, University of UTAD, 5000, Vila Real, Portugal

The process of mould design in the foundry industry has been based on the intuition and experience of foundry engineers and designers. To bring the industry to a more scientific basis the design process should be integrated with scientific analysis such as heat transfer. The production by foundry techniques is influenced by the geometry configuration, which affects the solidification conditions and subsequent cooling. Numerical simulation and/or experiments make possible the selection of adequate materials, reducing cycle times and minimizing production costs. The main propose of this work is to study the heat transfer phenomena in the mould considering the phase change of the cast-part. Due to complex geometry of the mould, a block unstructured grid and a generalized curvilinear formulation engaged with the finite volume method is described and applied. Two types of boundary conditions, diffusive and Newtonian, are used and compared. The developed numerical code is tested in real case and the main results are compared with experimental data. The results showed that the solidification time is about 6 seconds for diffusive boundary conditions and 14.8 seconds for Newtonian boundary conditions. The use of the block unstructured grid in combination with a generalized curvilinear formulation works well with the finite volume method and allows the development of more efficient algorithms with better capacity to describe the part contours through a lesser number of elements.

**Key Words :** Solidification, Heat Transfer, Phase Change, Finite Volume

## Nomenclature

### Roman

$B, C$  : Coefficients  
 $C_p$  : Heat capacity (J/kg °C)  
 $f_s$  : Solid fraction  
 $h$  : Newtonian heat transfer coefficient (W/m °C)  
 $J$  : Jacobean  
 $k$  : Thermal conductivity (W/m °C)  
 $q$  : Heat source (W/m<sup>3</sup>)  
 $t$  : Time (s)  
 $x, y$  : Cartesian coordinates

### Greek

$\beta$  : Cofactor  
 $\Delta h_f$  : Latent heat (J/kg)  
 $\phi$  : Temperature (°C)  
 $\rho$  : Density (kg/m<sup>3</sup>)  
 $\partial$  : Partial derivation  
 $\xi, \eta$  : Curvilinear coordinates system

### Subscripts

$a$  : Environment  
 $E$  : East  
 $f$  : Fusion  
 $i, j$  : Computational coordinates  
 $k$  : Iteration number  
 $l$  : Liquid or liquidus  
 $m$  : Mould  
 $N$  : North  
 $NE$  : Northeast

\* Corresponding Author,

**E-mail :** rouboa@utad.pt

**TEL :** +351-259-350317; **FAX :** +351-259-350356

Engineering Department, University of UTAD, 5000, Vila Real, Portugal. (Manuscript **Received** January 11, 2005; **Revised** August 8, 2005)

|       |                                      |
|-------|--------------------------------------|
| $NN$  | : North–North                        |
| $NNW$ | : Nor–Norwest                        |
| $NW$  | : Norwest                            |
| $P$   | : Central point of control volume    |
| $S$   | : South                              |
| $SE$  | : Southeast                          |
| $SS$  | : South–South                        |
| $SSE$ | : Sud–Southeast                      |
| $SW$  | : Southwest                          |
| $s$   | : Solid, solidus or solidified metal |
| $W$   | : West                               |

### Superscripts

|     |                                    |
|-----|------------------------------------|
| $i$ | : Number of Cartesian dimensions   |
| $j$ | : Number of curvilinear dimensions |
| $k$ | : Cofactor index                   |
| $m$ | : Cofactor index                   |
| $n$ | : Time iteration                   |

## 1. Introduction

The process of mould design in the foundry industry has long been based on the intuition and experience of foundry engineers and designers. To bring the industry to a more scientific basis the design process should be integrated with scientific analysis such as heat transfer, fluid flow and stress analysis.

Solidification modelling can be divided into three separate models, where each model is identified by the solution to a separate set of equations: heat transfer modelling which solves the energy equation; fluid–flow modelling which solves the continuity and momentum equations; and free–surface modelling which solves the surface boundary conditions. For a complete description of solidification modelling, all of these equations need to be solved simultaneously, but under special circumstances, the equations can be decoupled and modelled independently. This is the case for heat–transfer modelling, which has been widely used, and its application has significantly improved casting quality. However, heat–transfer modelling has many shortcomings, which must be taken into account whenever predictions are made (Teuk and Chang, 2003). These include a poor knowledge of the initial conditions, the

fact that fluid flow is not modelled, and that the predictions are based on experimental defect criteria (Swaminathan and Voller, 1996). Improvements can still be made in the area of the thermo–physical data relating to the metal–mould interface, phase changes and the temperature dependence of all thermo–physical data.

The major challenge to modelling the heat transfer of molten metal has been the phase change. To model such a phase change requires the strict imposition of boundary conditions. Normally, this could be achieved with a finite–element that is distorted to fit the interface. However, this is computationally expensive. Since the solid–liquid phase boundaries are moving, most classical fixed mesh finite–element or finite–difference schemes have not been able to maintain the correct boundary conditions.

To overcome the loss of boundary information we need to develop special treatments that recognize this discontinuity. The simplest is based upon the solid fraction in each computational cell. This fraction can be calculated in a variety of ways, either from: nucleation theory; linear extrapolation; the lever rule or the Scheil equation (Duff, 1999). Once this has been calculated it is necessary to account for the latent heat lost during solidification. This can be done in a variety of ways: a source term can be added to the energy equation; the specific heat can be modified; or a sensible–enthalpy formulation can be adopted (Sergey, 2002).

Complex geometries and distinct physical material properties are usual the case in a real casting scenario. The mesh generation using commercial software is often applied, when complex geometries are involved (Sergey, 2002; Pericleous, 1998). Otherwise, simple geometries are considered in order to validate the particular developed numerical code (Jungwoo and Haechon, 2004; Majchrzaka et al., 2000).

In this paper, the problem of the complex geometry is tackled using a block unstructured grid and a generalized curvilinear formulation engaged with the finite volume method. Two types of boundary conditions, diffusive (FV–k approach) and Newtonian (FV–h approach), are

used and compared to emphasize the error when the interface thermal resistance due to the gap between mould and cast part is neglected.

## 2. Mathematical model

The energy equation states that the rate of gain in energy per unit volume equals the energy gained by any source term, minus the energy lost by conduction, minus the rate of work done on the fluid by pressure and the viscous forces, per unit time. Assuming that : the fluid is isotropic and obeys Fourier's Law ; the fluid is incompressible and obeys the continuity equation ; the fluid conductivity is constant ; viscous heating is negligible, and since the heat capacity of a liquid at constant volume is approximately equal to the heat capacity at constant pressure, then the internal energy equation is reduced to the familiar heat equation, here written in curvilinear coordinates.

$$J \frac{\partial(\rho C_p \phi)}{\partial t} = \frac{\partial}{\partial x_j} \left[ \mathbf{k} \left( \frac{\partial \phi}{\partial \xi_m} \mathbf{B}^{mj} \right) \right] + \mathbf{J} \dot{q} \quad (1)$$

The curvilinear coordinates are defined for the transformation  $x_i = x_i(\xi, \eta, \zeta)$ ,  $j=1, 2, 3$ , and characterized by the Jacobean  $J$ . The coefficient  $B^{mj}$  in Eq. (1) is defined as :

$$B^{mj} = \beta^{kj} \beta^{km} = \beta^{1j} \beta^{1m} + \beta^{2j} \beta^{2m} \quad (2)$$

where  $\beta^{ij} = (-1)^{i+j} \det(J_{ij})$  represents the cofactor in Jacobean  $J$ .

The source term  $\dot{q}$  can be expressed as a function of effective solid material fraction  $f_s$ , metal density  $\rho$  and enthalpy variation in phase change  $\Delta h_f$ , called latent heat (Eliseu et al., 2003).

$$\dot{q} = \frac{\partial(\rho \Delta h_f f_s)}{\partial t} \quad (3)$$

The variable  $f_s$  can be decomposed in the following form :

$$\frac{\partial(f_s)}{\partial t} = \frac{\partial(f_s)}{\partial \phi} \frac{\partial(\phi)}{\partial t} \quad (4)$$

After some mathematical work the Eq. (1) the following expression is obtained,

$$J \frac{\partial \phi}{\partial t} \left( 1 - \frac{\Delta h_f}{C_p} \frac{\partial f_s}{\partial \phi} \right) = C_1 \frac{\partial \phi}{\partial \xi} + C_2 \frac{\partial \phi}{\partial \eta} + C_{11} \frac{\partial^2 \phi}{\partial \xi^2} + C_{12} \frac{\partial^2 \phi}{\partial \xi \partial \eta} + C_{22} \frac{\partial^2 \phi}{\partial \eta^2} \quad (5)$$

where the coefficients  $C_i$  and  $C_{ij}$  are determined by the following expressions :

$$C_1 = \frac{\partial(J^{-1})}{\partial \xi} B^{11} + \frac{\partial(J^{-1})}{\partial \eta} B^{12} + J^{-1} \left( \frac{\partial B^{11}}{\partial \xi} + \frac{\partial B^{12}}{\partial \eta} \right) \quad (6)$$

$$C_2 = \frac{\partial(J^{-1})}{\partial \xi} B^{21} + \frac{\partial(J^{-1})}{\partial \eta} B^{22} + J^{-1} \left( \frac{\partial B^{21}}{\partial \xi} + \frac{\partial B^{22}}{\partial \eta} \right) \quad (7)$$

$$C_{11} = J^{-1} B^{11} \quad (8)$$

$$C_{12} = J^{-1} (B^{21} + B^{12}) \quad (9)$$

$$C_{22} = J^{-1} B^{22} \quad (10)$$

## 3. Discretization

To tackle the problem of the complex geometry a block unstructured grid and a generalized curvilinear formulation engaged with the finite volume method were used.

To make easier the grid generation and the definition of the different physical properties of the mould and cast-part, the domain of interest was divided into 17 polygons with 4 vertices (sub-domains). After the definition of the four boundaries that define the contour of the sub-domain, it is needed to make the nodes distribution in each boundary. The same number of nodes in each boundary is required. The space between boundary-defined nodes does not have to be uniform. One of the advantages of this situation is the global reduction of the number of obtained points, with the increase of the space in zones where description can be made with lesser density of nodes (Thompson, 1985). However, it is necessary to care about brusque space variations. This can make impracticable the calculation of the local derivative, due to the continuity condition. The definition of the all coordinate lines in the interior of the domain is made by bilinear interpolation of the nodal positions defined in the boundaries resulting in the grid showed in the Fig. 2.

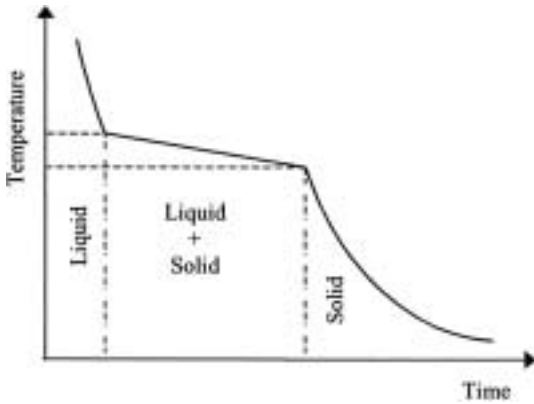


Fig. 1 Metallic alloy cooling curve

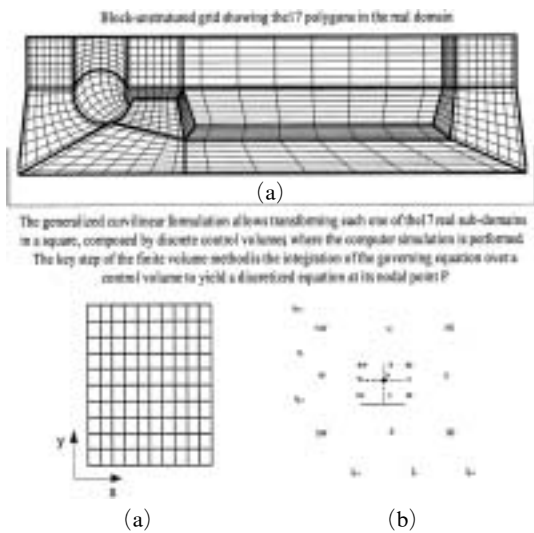


Fig. 2 Dcretization procedure: (a) block unstructured grid; (b) computational domain; (c) typical 2D control volume

Although the use of curvilinear coordinates imposes significant mathematical work in the model development, they allow a great comfort in the development of the computational code because in the transformed domain, the geometry is uniform, rectangular and time independent.

The space derivatives were approximated using the finite volume method for a nine-point computational cell like the one showed in the Fig. 2 where a geographical notation was used. Two levels of approximation are needed for surface integrals: the integral is approximated in terms of the variables values at one location on the cell

face, the midpoint point rule was used in this task; the cell face values are approximated in terms of the nodal values (control volume (CV) centres), the linear interpolation was used in this task. The volume integrals were approximated by a second-order approximation replacing the volume integral by the product of the mean value and the CV volume (Versteeg and Malalasekera, 1995). The time derivative was approximated by the implicit Euler scheme. The SIP (Strongly Implicit Procedure) was used as solver (Ferziger and Peric, 1999).

#### 4. Initial and Boundary Conditions

During the mould filing process the liquid material contacts the mould internal walls; consequently, the interface between metal and mould will have a certain thermal resistance that occurs because the mould internal wall is not completely wet by the liquid (O'Mahoney and Browne, 2000). The mould internal roughness generates a micron superficial geometry that propitiates the developing of few contact points intercalated by regions of physical separation between metal and mould.

The material contraction provokes an increase of physical separation between the solid material and the mould. In these conditions, the heat transfer in the interface between metal and mould is given by:

- (1) conduction in contact points and through the gases imprisoned by the created spaces;
- (2) convection and radiation between the two separate surfaces.

The material type, surface condition of the mould, quality of the desired superficial finishing and mould temperature controls the superficial roughness. In metal mould solidification, the parameters of thermal behavior of the interface between metal and mould rule the heat transfer and determine the solidification progression. The heat flux through an interface will be the result of the transfer modes combination that may co-exist:

- (1) Conduction through the applied coating

layer ;

(2) Conduction through the gases of the gap between the part and the mould ;

(3) Radiation between the surfaces of the part and the mould through the same gap.

The heat transfer coefficient value varies in function of several factors, namely :

(1) thickness and thermal conductivity of coating layer ;

(2) form and dimensions of the part and mould ;

(3) geometry of the gap between different sections in contact, which is dependent of the material natural thermal expansion ;

(4) surface finishing of the different interfaces ;

(5) state of agitation of the surrounding air (in the case of heat transfer to the environment).

Different possibilities must be considered for heat transfer conditions on boundaries :

(1) perfect contact (Monteiro, 1996):

$$\left(\frac{\partial\phi}{\partial\mathbf{n}}\right)_{m_1} = \left(\frac{\partial\phi}{\partial\mathbf{n}}\right)_{m_2} \text{ and } \phi_{m_1} = \phi_{m_2} \quad (11)$$

for boundaries defined with continuous material ;

(2) diffusion heat transfer Eq. (12) in the FV-k approach, and Newtonian heat transfer Eq. (13) for the FV-h approach,

$$k_m \left(\frac{\partial\phi}{\partial\mathbf{n}}\right)_m = k_s \left(\frac{\partial\phi}{\partial\mathbf{n}}\right)_s \quad (12)$$

$$\mathbf{k}_m \left(\frac{\partial\phi}{\partial\mathbf{n}}\right) = h_i (\phi_m - \phi_s) \quad (13)$$

applied to boundaries between the exterior wall of the part and in the interior wall of the mould ;

(3) convective heat transfer for the exterior boundary of the system which contacts the environment Eq. (14).

$$k_m \left(\frac{\partial\phi}{\partial\mathbf{n}}\right)_m = h_a (\phi_m - \phi_a) \quad (14)$$

The liquidus temperature is used as initial condition for the domains that form the cast-part.

The initial temperature field in the mould is the result of the cooling simulation with the mould closed and empty. For this simulation, 300°C is

**Table 1** Physical properties

| Physical property               | Al 12Si | Grey Cast-Iron |
|---------------------------------|---------|----------------|
| Density [kg/m <sup>3</sup> ]    | 2670    | 7230           |
| Thermal conductivity [W/m °C]   | 185     | 38             |
| Thermal heat capacity [J/kg °C] | 1260    | 750            |
| Latent heat [kJ/kg]             | 395     | —              |
| Liquidus temperature [°C]       | 585     | —              |
| Solidus temperature [°C]        | 575     | —              |

**Table 2** Newtonian heat transfer coefficients at interfaces (Monteiro, 1996)

| Interface      | Newtonian Heat transfer coefficient [W/m <sup>2</sup> °C] |
|----------------|---|
| D1/D2          | $h_i=2500$  |
| D1/D3          | $h_i=2500$  |
| D1/D4          | $h_i=2500$  |
| D2/D3          | $h_i=500$   |
| D3/D4          | $h_i=600$   |
| D2/environment | $h_a=150$   |
| D3/environment | $h_a=150$   |

used as initial temperature, and the results are obtained 60 seconds after.

In this simulation the interface with the empty cavity was considered adiabatic. The small circulation and the reduced thermal capacity of the air justify this assumption.

The values of the physical properties of the involved materials used in the numerical simulation are indicated in Tables 1 and 2.

All this method was implemented using the programming language FORTRAN and the data post-processing carried out with Tecplot.

## 5. Results Discussion

The initial temperature field of Fig. 3 shows that the temperature decreases as long the distance

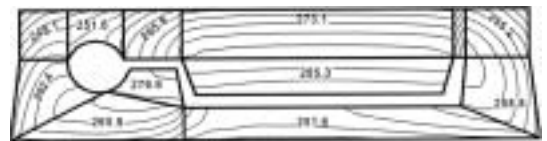


**Fig. 3** Initial temperature field in the mould

to the environment decreases. The corners of the superior part of the mould have lower temperature values than the inferiors, what it is perfectly realistic due to its lesser dimensions.

The simulation of the temperature field for the set part/mould was carried out for two situations. First, considering diffusion heat transfer and second, considering Newtonian heat transfer.

## 6. Diffusion Heat Transfer at Interface Part/Mould

In this approach, only diffusion heat transfer is considered. The relation of thermal conductivities of the involved materials is the coefficient of proportionality between the heat flux and the temperature differences.

The end of the solidification occurs after 6 seconds of cooling, which means that all the part material has below of the solidus temperature ( $575^{\circ}\text{C}$ ). This temperature field is shown in Figs. 4~5 for the part and mould, respectively. The areas of slighter thickness are the coldest ones. In opposite, the hottest areas have larger dimensions. The mould highest temperature occurs, as expected, near to the part.

Making a comparison between the temperature field in the mould at the end of solidification (Fig. 5) and the initial temperature field of Fig. 3,



**Fig. 4** Part temperature field after at the end of solidification (6 seconds of cooling) considering diffusion heat transfer at interface part/mould

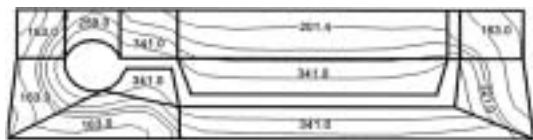


**Fig. 5** Mould temperature field at the end of solidification (6 seconds of cooling) considering diffusion heat transfer at interface part/mould.

it is verified that the coldest zones continue to be the superior mould corners. However, the superior left corner, because of its proximity to the part hottest zone, has a temperature level superior to the initial.

## 7. Newtonian Heat Transfer at Interface Part/Mould

In this approach it was used a Newtonian heat transfer coefficient to have into account the gap between the part and the mould. The end of the solidification occurs after 14,8 seconds of cooling (Fig. 6). A discontinuity in the temperature values in the interfaces where the Newtonian heat transfer is verified.

High temperature gradients were verified in the cylindrical zone of the cast part. This behavior allows confirm that the solidification starts from the surrounding metal and finishes in the centre of the cylinder.

The extremity on the right-side of the cast part is the coldest zone at the end of solidification. The distance to the hottest fraction of the cast part and its thin dimensions explains such behavior.

The comparison between the mould temperature field at the end of solidification (Fig. 7) and the initial temperature field shows that the coldest zones are the superior mould corners.



**Fig. 6** Part temperature field at the end of solidification (14,8 seconds of cooling) considering Newtonian heat transfer at interface part/mould

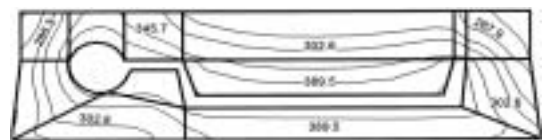


**Fig. 7** Mould temperature field at the end of solidification (14,8 seconds of cooling) considering Newtonian heat transfer at interface part/mould

### 8. Model Validation

The comparison between experimental and numerical data is made for the points where the thermocouples were placed (see Fig. 8).

Making an analysis to the Figs. 9-11 we can notice that :

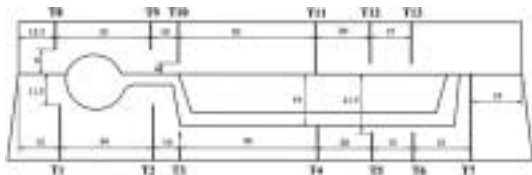


**Fig. 8** Used positions of the thirteen thermocouples in the cross-section to obtain experimental temperature values

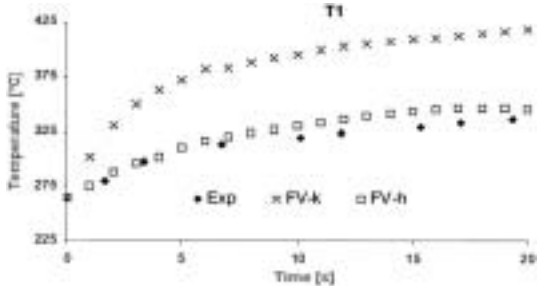


**Fig. 9** Comparison with experimental (Exp) and numerical data using the finite volume method with Newtonian boundary conditions (FV-h) and with diffusive boundary conditions (FV-k) for thermocouple T1

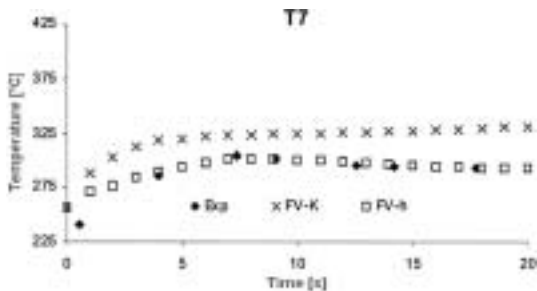


**Fig. 10** Comparison with experimental (Exp) and numerical data using the finite volume method with Newtonian boundary conditions (FV-h) and with diffusive boundary conditions (FV-k) for thermocouple T7

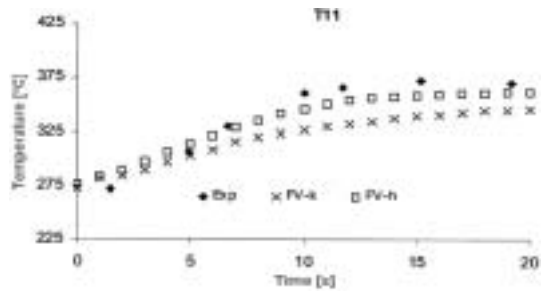


**Fig. 11** Comparison with experimental (Exp) and numerical data using the finite volume method with Newtonian boundary conditions (FV-h) and with diffusive boundary conditions (FV-k) for thermocouple T11

(1) the numerical results obtained by the first approach (FV-k) follow the behavior of the experimental values, but with unacceptable discrepancy ;

(2) the numerical results obtained by the second approach (FV-h) shows a very good agreement with the experimental values.

### 9. Conclusions

The suitable agreement of the numerical results FV-h with the experimental measurements allows the validation of the information supplied by the developed model. The discrepancy verified between FV-k and FV-h approaches allows confirming that is the interface thermal resistance that governs the evolution of the temperature fields in metallic mould.

The use of the block unstructured grid in combination with a generalized curvilinear formulation works well with the finite volume method and allows the development of more efficient algorithms with better capacity to describe the contours through a lesser number of elements and without geometric limitations imposed for the involved particular geometry.

### References

Aavatsmark, I., Barkve, T., Boe, O., Mannseth, T., 1998, "Discretization on Unstructured Grids for Inhomogeneous, Anisotropic. Part I: Deri-

- vation of the Methods,” *SIAM Journal of Numerical Analysis*, Vol. 19, No.5, pp. 1700~1716. (Journal)
- Duff, E. Stanley, 1999, *Fluid Flow Aspects of Solidification Modelling: Simulation of Low Pressure Die Casting*, Ph.D Thesis, University of Queensland, Australia. (Thesis)
- Eliseu Monteiro, Abel Rouboa and Caetano Monteiro, 2003, “Heat Transfer Simulation in the Mould with Generalized Curvilinear Formulation,” *ASME Residual Stress, Fitness-for-Service, and Manufacture Processes*, Vol. 464, pp. 231~237. (Book)
- Ferziger, J. H., Perić, M., 1999, *Computational Methods for Fluid Dynamics*. 2<sup>nd</sup> edition, Springer Verlag, Berlin, Heidelberg, New York. (Book)
- Jungwoo Kim, Haecheon Choi, 2004, “An Immersed-Boundary Finite-Volume Method for Simulation of Heat Transfer in Complex Geometries,” *KSME International Journal*, Vol. 18, No. 6, pp. 1026~1035. (Journal)
- Majchrzaka, E., Mochnackib, B., Szopab, R., 2000, “Application of the Boundary Element Method for the Numerical Modelling of the Solidification of Cylindrical and Spherical Castings,” *Journal of Materials Processing Technology*, 106, pp. 99~106. (Journal)
- Monteiro, A. A. C., 1996, *Estudo do Comportamento Termico de Moldacoes Metalicas para Fundicao Aplicando o Metodo das Diferencas Finitas Generalizadas*, Ph.D Thesis, University of Minho, Portugal. (Thesis)
- O’Mahoney, D. and Browne, D. J., 2000, “Use of Experiment and an Inverse Method to Study Interface Heat Transfer During Solidification in the Investment Casting Process,” *Journal of Experimental Thermal and Fluid Science*, 22, pp. 111~122. (Journal)
- Pericleous, K. A., Moran, G. J., Bounds, S. M., Chow, P. and Cross, M., 1998, “Three-Dimensional Free Surface Modelling in an Unstructured Mesh Environment for Metal Processing Applications,” *Applied Mathematical Modelling*, 22, pp. 895~906. (Journal)
- Sergey V. Shepel, Samuel Paolucci, 2002, “Numerical Simulation of Solidification of Permanent Mold Castings,” *Journal of Applied Thermal Engineering*, 22, pp. 229~248. (Journal)
- Swaminathan, C. R. and Voller, V. R., 1996, “Towards a General Numerical Scheme for Solidification System,” *International Journal of Heat and Mass Transfer*, 40 :2859. (Journal)
- Teuk, M. Y. and Chang, N. K., 2003, “A Numerical Analysis of Molten Steel Flow under Applied Magnetic Fields in Continuous Casting,” *KSME International Journal*, Vol. 17, No. 12, pp. 2010~2018. (Journal)
- Thompson, J. F., Warsi, Z. U. A. and Mastin, C. W., 1985, “Numerical Grid Generation, Foundations and Applications,” *Elsevier Science Publishing Co.* (Book)
- Usmani, A. S., Cross, J. T. and Lewis, R. W., 1992, “A Finite Element Model for the Simulations of Mould Filling in the Metal Casting and the Associated Heat Transfer,” *International Journal for Numerical Methods in Engineering*, 35, pp. 787~806. (Journal)
- Voller, V. R., Brent, A. D. and Prakash, C., 1989, “The Modelling of Heat, Mass and Solute Transport in Solidification Systems,” *International Journal of Heat and Mass Transfer*. (Journal)
- Versteeg, H. K. and Malalasekera, W., 1995, *An Introduction to Computational Fluid Dynamics, the finite volume method*, Prentice Hall. (Book)